Available online at www.sciencedirect.com
SCIENCE DIRECT®
Journal of Chromatography A, 990 (2003) 23–33
JOURNAL OF CHROMATOGRAPHY A
www.elsevier.com/locate/chroma

Capillary zone electrophoresis in wide bore capillary tubes with fiber-coupled diode array detection

Stanislav Strašík, Mariana Danková, Markéta Molnárová, Eva Ölvecká, Dušan Kaniansky*

Department of Analytical Chemistry, Faculty of Natural Sciences, Comenius University, Mlynská Dolina CH-2, SK-84215 Bratislava, Slovak Republic

Abstract

This feasibility study deals with the use of a wide bore (320 μm I.D.) capillary tube for the detection and identification of capillary zone electrophoresis (CZE) analytes by optical fiber-coupled diode array detection. A 250-μm mean effective pathlength of the detection cell with an inherently enhanced photon flux through the cell were significant contributors in reaching 0.2–1 μmol/l concentration detectabilities of the CZE analytes by this combination. Experiments with model analytes (*p*-sulfanilic, sorbic and naphthalene-2-sulfonic acids, tryptophan and asulam) revealed that spectral confirmations of their identities were still possible when their concentrations in the loaded samples (200 nl) were 1–5 μmol/l. Here, chemometry procedures (target transformation factor analysis, fixed size moving window-target transformation factor analysis, fixed size moving window-evolving factor analysis and orthogonal projection approach) employed in the data processing effectively contributed to reliable confirmation of the identities of the analytes also in critical situations (e.g. peak overlaps). The CZE separations were carried out in tandem-coupled columns of identical I.D. This made it possible to use, in the first column of the tandem, carrier electrolyte solutions that provide the desired separative effects, while in the second (detection) column the compositions of the carrier electrolyte solutions employed could reflect favorable conditions for obtaining spectral data. Mixtures containing model constituents at significantly differing concentrations and Maillard's reaction products spiked with tryptophan enantiomers were employed in experiments aimed at assessing practical applicabilities and limits of the present approach to the analysis of samples characterized by complex ionic matrices.

Keywords: Diode array detection; Detection, electrophoresis; Chemometrics; Naphthalene-sulfonic acids; Asulam; Sorbic acid; Sulfanilic acid

1. Introduction

A need for unambiguous identification of trace capillary zone electrophoresis (CZE) analytes by combining their spectral and migration data is apparent, especially when samples characterized by complex matrices are to be analyzed [1]. Currently, on-column coupled ultraviolet and visible spectrometry is a preferred optical spectral technique that is employed for identification purposes in CZE (see, e.g., Refs. [2–12]). Other spectral identification techniques are either applicable to a limited group of analytes (e.g. fluorescence spectrometry [13]) or they are sufficiently sensitive only in combination with electrophoretic methods that concentrate the sample constituents (e.g. Raman spectroscopy [14,15] and nuclear magnetic resonance [16,17] combined with isotachophoresis (ITP)).

*Corresponding author. Tel.: +421-2-6029-6379; fax: +421-2-6542-5360.
E-mail address: kaniansky@fns.uniba.sk (D. Kaniansky).

0021-9673/02/$ – see front matter
doi:10.1016/S0021-9673(02)01813-7

At present, CZE separations are carried out almost exclusively in capillary tubes of 50–75 μm I.D. Although favoring very high separation efficiencies, the separations in capillaries of such dimensions are, in general, characterized by moderate concentration limits of detection (cLODs) for the separated constituents. For example, UV absorbance detectors, typically, fail to detect the light-absorbing constituents when these are present in the loaded samples at low μmol/l concentrations [2]. Therefore, approaches that use extended absorbance pathlengths in the detection cells (e.g. Z-cell [18], U-cell [19] and bubble cell [4] designs, a multireflection cell [20] and axial-beam absorption [21]) or averaged electropherograms, acquired by an array of independently treated sensors placed along the capillary [22], were developed to reach sub-μmol/l concentration detectabilities in CZE. The acquisition of light absorption spectra with the aid of diode array detection (DAD) systems make use of the extended pathlength in the detection cell as well (see, e.g., Refs. [4,5,23]). In this context it is necessary to note a contribution of the extended pathlength (slit width) to the band broadening [24] as this may be less tolerable, for example, in the separations performed in shorter capillary tubes.

Fiber optics offers some apparent advantages in single- and multiwavelength photometric absorbance detection in CZE [10,25–32]. Here, the above sensitivity limits, even more crucial than in the on-column detector designs [31], need to be taken into account as well. Detection performance data as obtained with the aid of the optical fiber-based detector in the tubes of 30–100 μm I.D. [31] indicate that the use of tubes of larger I.D. offers one way of reaching improved concentration detectabilities. This agrees with the results provided by current on-column photometric detectors in the capillary tubes of larger I.D. (see, e.g., Refs. [33–42]). In this context it seems appropriate to note that an overall benefit linked with the use of wide bore capillaries with fiber optic sensing, is in a combination of an enhanced sample loadability [38] with an increased absorbance pathlength in the detection cell (without increasing the slit width of the cell) and an enhanced light flux through the sensing part that reduces the effect of shot noise [2,10,43]. Here, however, contrary to the use of capillaries of 50–75 μm I.D., more attention has to be paid to the thermal dispersive effects [24].

In our previous work we showed some detection and identification possibilities of DAD (coupled by optical fibers to the CZE column of a 320 μm I.D.) in CZE with on-line ITP sample pretreatment [44]. Using this CE combination we benefited, mainly, from the sample pretreatment capabilities of ITP and a high sample loadability of the ITP–CZE separation system. Due to this, we could identify the test analyte (orotic acid) in diluted urine matrices by DAD at sub-μmol/l concentrations using only simple data processing means. This work was aimed at enhancing the detection and identification capabilities of the fiber-coupled DAD via a design of the CZE column and the use of chemometry procedures that more effectively process the acquired spectral data [45].

2. Experimental

2.1. Instrumentation and the DAD data processing

An ITAChrom EA-101 capillary electrophoresis analyzer (J&M, Aalen, Germany) was used in this work. Its separation unit was equipped with a tandem-coupled CZE column (Fig. 1) constructed in this laboratory. The column was provided with 320 μm I.D. (410 μm O.D.) fused-silica capillary tubes (J&W, Folsom, Canada) coupled in a bifurcation block [46]. The length of the first capillary of the tandem (from the injection valve to the bifurcation block) was 120 mm and the length of the second capillary (from the bifurcation block to the detector) was 70 mm. The sample was injected by a 200-nl internal sample loop of the CZE injection valve of the analyzer.

A TIDAS multiwavelength photometric absorbance diode array detector (J&M) was connected to an on-column detection cell, mounted on the second CZE column of the tandem, via optical fibers (J&M). The cell construction followed a previous design from this laboratory [47]. The detector operated under the following settings: (1) scanned wavelength range, 200 to 350 nm; (2) integration time, 15 ms; (3) scan interval, 1.25 s; (4) number of accumulations, 80. The spectral data were acquired by a Spectralys program (version 1.81, J&M). Data processing procedures of the Spectralys program (background corrections, smoothing, calculations of the

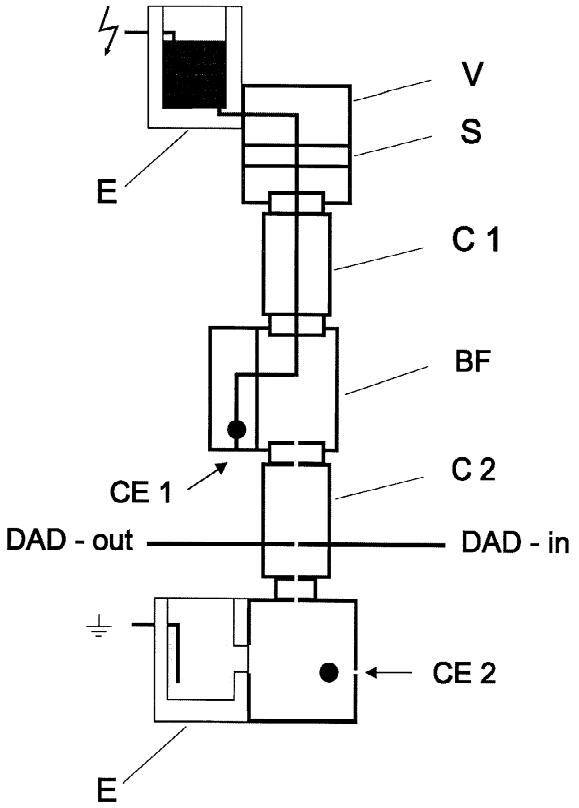

Fig. 1. CZE separation unit with a hydrodynamically closed separation compartment provided with the tandem-coupled columns. E, electrode vessels with the driving electrodes dipped into the corresponding carrier electrolyte solutions; V, injection valve with a 200-nl internal sample loop in a rotating disk (S); C1, C2, separation (C1) and detection (C2) columns, provided with 320 μm I.D. fused-silica capillary tubes, coupled in the bifurcation block (BF); CE1, CE2, valves for filling the columns C1 and C2 with the carrier electrolyte solutions, respectively; DAD-in and DAD-out, illuminating and light collecting optical fibers (500 μm cores), respectively. For further details see the Experimental section.

Pearson correlation coefficients and match factors), chemometry procedures described in the literature (target transformation factor analysis [45], TTFA; fixed size moving window-evolving factor analysis [45,48,49], FSW-EFA; orthogonal projection approach [45,48,50], OPA) and a TTFA procedure modified in this laboratory (fixed size moving window target transformation factor analysis, FSW-TTFA) were used in the spectral data processing. The programs for these procedures were written in the laboratory using Mathematica for Windows (version 4.0, Wolfram, Champaign, IL, USA).

2.2. Electrolyte solutions and samples

Chemicals used for the preparation of the electrolyte solutions and the solutions of model samples were obtained from Sigma–Aldrich (Seelze, Germany), Serva (Heidelberg, Germany), Reanal (Budapest, Hungary), Lachema (Brno, Czech Republic) and Merck (Darmstadt, Germany).

Methylhydroxyethylcellulose 30 000 (Serva), purified on a mixed-bed ion-exchanger (Amberlite MB-3, Merck), was used as a suppressor of electroosmotic flow (EOF). It was added to the carrier electrolyte (Table 1).

Water demineralized by a Pro-PS water purification system (Labconco, Kansas City, KS, USA), and kept highly demineralized by a circulation in a Simplicity deionization unit (Millipore, Molsheim, France), was used for the preparation of the electrolyte and sample solutions. The electrolyte solutions were filtered by disposable syringe membrane filters of 0.8-μm pore sizes (Sigma) before use.

A group of test analytes (*p*-sulfanilic, sorbic and naphthalene-2-sulfonic acids, tryptophan and methyl(4-aminosulfonyl)carbamate (asulam)), obtained from the above suppliers, their mixtures with co-migrating constituents and their mixtures with Maillard's reaction products of glycine and xylose [51] served as samples in our experiments.

3. Results and discussion

Favorable CZE separating conditions can be in some instances contradictory to those leading to sensitive photometric absorbance detection of the analytes. In such instances, it is advantageous to perform the CZE separations in sequences of the carrier electrolyte solutions as provided, for example, by a partial filling technique [52]. This technique, effective in hydrodynamically opened separation systems, however, is not easily employed in CE instruments designed for CZE separations with a hydrodynamically closed separation system [33,34,38] as favored in the separations in wide bore tubes. To overcome this drawback of the closed systems we favored in this work the use of tandem-

Table 1
Electrolyte systems

Parameter	Electrolyte system no.			
	1a	1b	1c	2
Solvent	Water	Water	Water	Water
Carrier anion	MES	MES	MES	β-Ala
Concentration (m*M*)	50	100	150	40
Counter-ion	ε-ACA	ε-ACA	ε-ACA	AMM
EOF suppressor	MHEC	MHEC	MHEC	MHEC
Concentration (%, w/v)	0.2	0.2	0.2	0.2
Chiral selector	–	–	–	α-CD
Concentration (m*M*)	–	–	–	120
pH	5.2	5.2	5.2	9.7

MES, 2-[*N*-morpholino]ethanesulfonic acid; ε-ACA, 6-amino-*n*-caproic acid; MHEC, methylhydroxyethylcellulose; β-Ala, β-alanine; α-CD, α-cyclodextrin; AMM, 2-amino-2-methyl-1,3-propanediol.

coupled columns (Fig. 1). Here, a pair of 320 μm I.D. columns was coupled in the bifurcation block as originally designed for the column-coupling ITP separations [46]. An independent filling of the columns (see Fig. 1) made possible the CZE separations either in identical carrier electrolytes or in sequences of the carrier electrolytes of specific functions.

3.1. Detectabilities and identification of the analytes in a 320 μm I.D. tube

For reasons discussed in detail in the work by Lindberg et al. [31] fiber-coupled photometric absorbance detectors provide less favorable detectabilities of CZE analytes than their on-column counterparts. From CZE experiments performed with the present fiber-based detection system it is apparent (see illustrative electropherograms in Fig. 2) that the use of a wide bore (320 μm I.D.) capillary tube led to lower concentration detectabilities of the analytes in comparison to those considered as current cLOD in on-column photometric absorbance detection in tubes of 50–75 μm I.D. [2]. However, this is understandable as the detection cell employed in our experiments was characterized by a 250-μm mean effective pathlength [2] and an inherently higher photon flux through the cell and, consequently, reduced effects of the shot noise on the detection [2,10,43].

The DAD spectra acquired at the peak apexes of the test analytes, when these were loaded at about 10 μmol/l concentrations (see Fig. 3), required background corrections and smoothing to match the reference spectra obtained under identical working conditions for 100 μmol/l concentrations of the

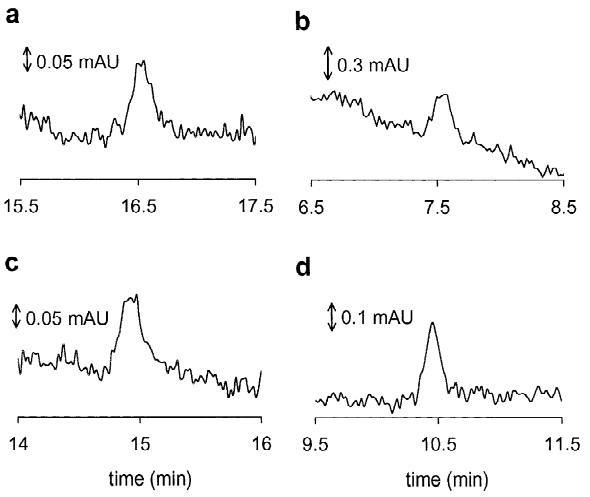

Fig. 2. Electropherograms from the CZE runs with the test analytes present in the loaded samples at concentrations approaching to their cLOD values attainable, at particular detection wavelengths, by the optical fiber-coupled DAD system. The analytes were loaded into the separation system by a 200-nl volume loop of the injection valve. (a) Asulam (256 nm), present in the sample at a 0.5 μmol/l concentration; (b) naphthalene-2-sulfonic acid (225 nm), present in the sample at a 0.3 μmol/l concentration; (c) sorbic acid (255 nm), present in the sample at a 0.5 μmol/l concentration; (d) sulfanilic acid (248 nm), present in the sample at a 0.5 μmol/l concentration. The separation and detection columns of the tandem were filled with an identical carrier electrolyte solution (the system no. 1b, in Table 1). The driving current was stabilized at 50 μA.

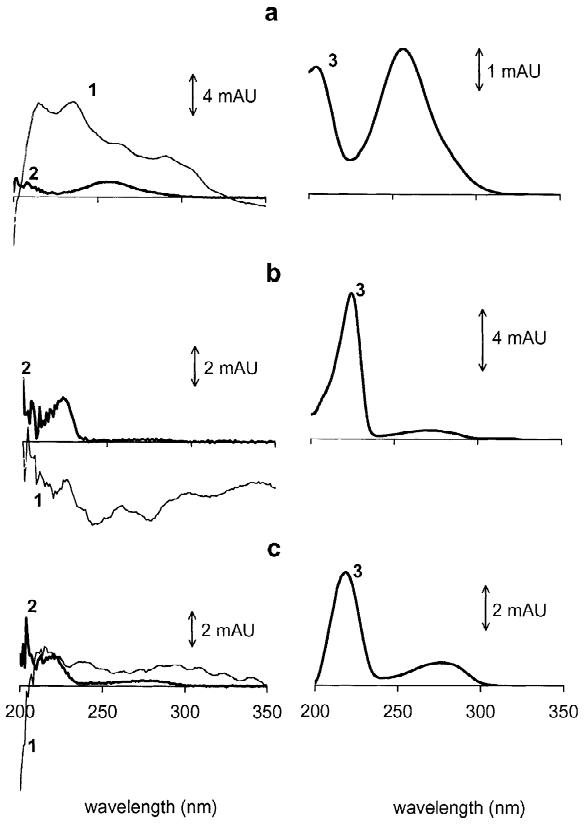

Fig. 3. Spectra acquired from the CZE runs with the test analytes by the fiber-coupled DAD system. (a) Asulam [raw (1) and background corrected and smoothed (2) spectra for a 5 μmol/l concentration of the analyte; a background corrected and smoothed spectrum for a 10 μmol/l concentration of the analyte (3)]; (b) naphthalene-2-sulfonic acid [raw (1) and background corrected and smoothed (2) spectra for a 1 μmol/l concentration of the acid; background corrected and smoothed spectrum for a 10 μmol/l concentration of the acid (3)]; (c) tryptophan [raw (1) and background corrected and smoothed (2) spectra for a 5 μmol/l concentration of tryptophan; background corrected and smoothed spectrum for a 20 μmol/l concentration of tryptophan (3)]. The spectra of asulam and naphthalene-2-sulfonic acid were acquired from their peak apexes from the CZE runs performed in the electrolyte system no. 1b (Table 1) while the ones of tryptophan were acquired in the electrolyte system no. 2 (without α-CD). The driving current was stabilized at 50 μA.

analytes (neither background corrections nor smoothing was applied for the reference spectra). For lower concentrations of the analytes, however, only processing of the raw spectral data by TTFA led to match factors confirming the identities of the analytes with high certainties (Table 2).

Concentration limits at which the TTFA method is still effective in confirmation of identities of the analytes under our DAD detection conditions were estimated from the CZE runs performed with model samples containing 0.1–1000 μmol/l concentrations of the test analytes and samples containing, besides the analytes, also co-migrants at comparable concentrations. Transformed Pearson correlation coefficients [the transformation used the form, $-\log(1-r+10^{-4})$, to eliminate discontinuities for the values of $r=1$] obtained from these experiments and plotted against the concentrations of the analytes in the loaded samples are given in Fig. 4. The plots, expressing the spectral matches provided by the TTFA procedure, had characteristic courses. From these courses it is apparent that the transformed Pearson correlation coefficient for a particular analyte decreased only very slightly with a decreased concentration of the analyte down to a certain critical concentration (''limit of identification''). Below this concentration a sharp decrease of the correlation coefficient was typical and, in addition, its value did not depend on the concentration of the analyte when this was present in the loaded sample at a lower concentration. The plots (a) and (b) in Fig. 4 show that co-migrating interferents did not influence these courses significantly.

3.2. Enhancing detectabilities of the analytes in the tandem-coupled columns

The concentration of the carrier ion of the carrier electrolyte solution determines, in accordance with the Kohlrausch regulating function, the concentrations of the separated constituents in CZE [34]. As the situation in each of the tandem-coupled columns is governed by its own Kohlrausch regulating function, a higher concentration of the carrier ion in the detection column, concentrating the separated constituents, provide conditions for higher qualities of the spectral data acquired by DAD. The analytical possibilities of such an approach were investigated in a context with the detection and identification of trace impurities present in the preparation of one of the test analytes (asulam). Electropherograms obtained from the acquired spectral data in the runs with identical and different concentrations of the

Table 2
Impact of the processing of the acquired spectral data on the Pearson correlation coefficients and match factors

Analyte	Concentration (μmol/l)	Processing of the acquired spectral data			
		Background correction and smoothing		TTFA	
		r	Match factor	*r*	Match factor
Asulam	5	0.98108	962.51	0.99985	999.70
NAPH[a]	1	0.84699	717.39	0.99969	999.37
Tryptophan	4	0.81091	657.58	0.99971	999.42

TTFA, target transformation factor analysis; *r*, Pearson's correlation coefficient; match factor = $1000 \times r^2$.
[a] NAPH, naphthalene-2-sulfonic acid.

carrier ion in the coupled columns (Fig. 5) clearly demonstrate enhanced detectabilities of the trace constituents linked with the use of this approach. Improved spectra of the trace impurities were acquired in this way as well (Fig. 6).

The electropherograms (Fig. 5), the spectra of impurities (Fig. 6) and data given in Table 3 indicate that the concentrating effects attainable in the detection column of the tandem can be beneficial in acquiring the spectral data for the trace analytes present in the loaded samples down to about 0.01% concentrations (relative to the detected sample macroconstituent). On the other hand, it is necessary to stress that the concentrating effect in the detection column is not restricted to the separated constituents and the carrier ions entering this column are concentrated as well. Due to this, the resolutions of some constituents attained in the separation column of the tandem were reduced (imp1–imp3 in Fig. 5b) or almost totally lost (x in Fig. 5b). Undoubtedly, this may limit a practical utility of this approach.

3.3. Identification of trace analyte overlapped by matrix constituents

An indirect identification potential of the present DAD method with the data processing by FSW-EFA and OPA was assessed for situations relevant to overlaps of the peak of the trace analyte by the matrix constituents. Here, a model mixture contained naphthalene-2-sulfonic acid at a 0.5 μmol/l concentration, while other acids (2,5-dichlorobenzenesulfonic, *p*-aminosalicylic and 2,4-dinitrobenzoic acids), representing the matrix constituents, were present in the mixture at 200-times higher concentrations. An illustrative electropherogram obtained from the CZE run with the model mixture of this composition is given in Fig. 7. The output data, eigenvalues, obtained from the FSW-EFA processing of the corresponding spectral data are plotted in Fig. 8. The first plot of the eigenvalues (E1, in Fig. 8) represented an envelope of the electropherogram. A dominant peak in the E2 plot corresponded to the overlap of the peaks of 2,5-dichlorobenzenesulfonate and *p*-aminosalicylate. Small asymmetric peaks in this plot, corresponding to rising and falling edges of the peaks on the electropherogram, were ascribed to contributions of the carrier electrolyte. Therefore, their shapes were (likely) linked with concentration changes of the carrier electrolyte along the zones of the separated constituents. A peak marked with an asterisk in the E3 plot was attributed to the trace analyte (this was confirmed by the CZE runs with and without naphthalene-2-sulfonate in the sample) while interpretations of the remaining two were not clear. The E4 plot and the eigenvalue plots of higher indices corresponded to the detection noise. In this context, it is to be noted that the courses of the eigenvalues became more complex with an increasing number of constituents and their assignments were not unambiguous.

The outputs for the same spectral data processed by the OPA procedure are given in Fig. 9. Here, P1–P6 are dissimilarity plots (changes in the dissimilarity courses in dependence on the references employed). An average spectrum calculated for the investigated time interval on the electropherogram served as a reference in the calculation of the P1 plot. An arrow in this plot indicates a position of the reference taken for the calculations of a subsequent (P2) plot. This interactive procedure continued till the noise level was reached. The total number of

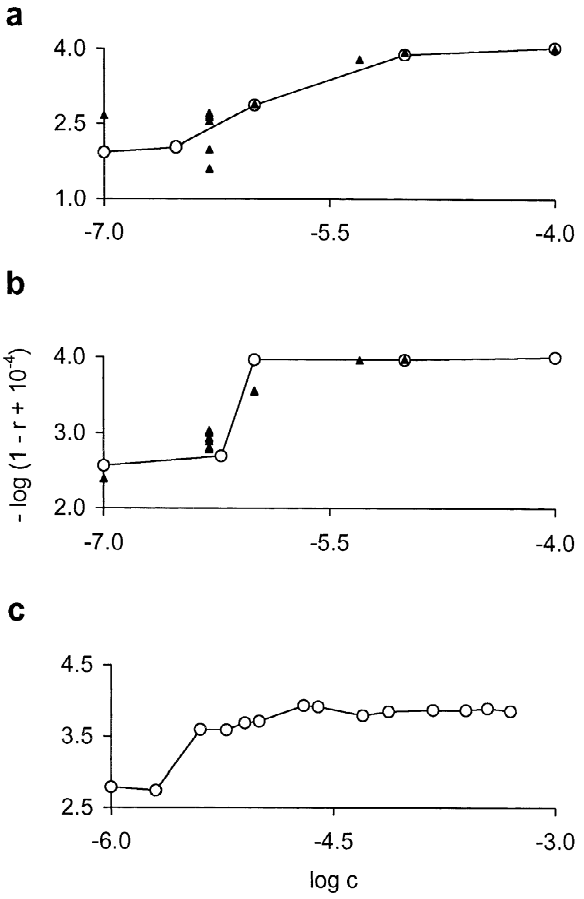

Fig. 4. Dependences of logarithmically transformed values of the Pearson correlation coefficients of the test analytes on their concentrations in the loaded samples with the TTFA data processing applied. (a) Asulam (*o*-aminobenzoic acid and *N*-acetyltryptophan served as comigrants); (b) naphthalene-2-sulfonic acid (2,5-dichlorobenzenesulfonic and *p*-aminosalicylic acids were used as comigrants); (c) tryptophan. ○, data points obtained from the runs with the samples containing only the analytes (the points are interconnected by full lines); ♦, data points from the runs in which the samples contained beside the analytes also the above comigrants (present in the loaded samples at concentrations comparable with those of the analytes). The runs with asulam and naphthalene-2-sulfonic acid were carried out in the electrolyte system no. 1b (Table 1) while the ones with tryptophan were carried out in the electrolyte system no. 2 (without α-CD). The driving current was stabilized at 50 μA.

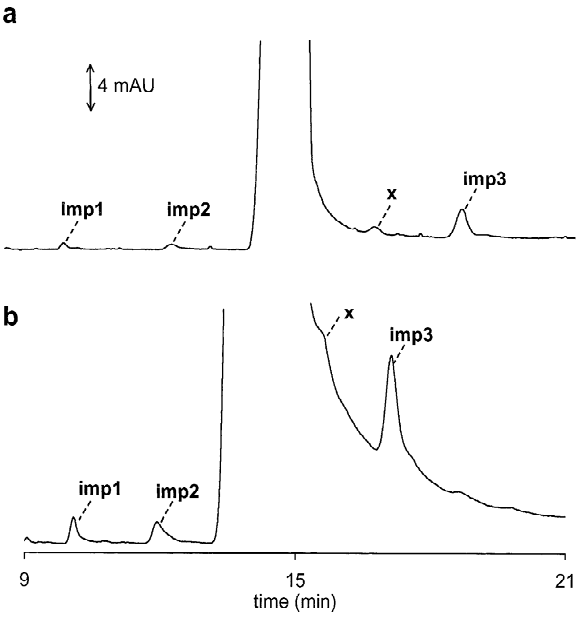

Fig. 5. Electropherograms (256 nm) from the CZE separations of asulam in the tandem-coupled columns with different carrier electrolyte solutions in the detection column. (a) The separation and detection performed in the electrolyte system no. 1a (Table 1); (b) the separation performed in the electrolyte system no. 1a was followed by the detection in the electrolyte system no. 1c (Table 1). In both instances the concentration of asulam in the loaded sample was 5 m*M*. The driving current was stabilized at 50 μA. imp1–imp3, and x are impurities originating from the asulam preparation.

plots was equal to the number of analytes plus one (corresponding to the carrier electrolyte; in our instance it was taken from a position marked by an asterisk in P4). Each of the references (spectra of mixtures) was assumed to provide maximum information on one of the separated constituents and the presence of naphthalene-2-sulfonate (marked with an asterisk in Fig. 9) was detected in the P5 plot.

3.4. Identification of enantiomers present in a complex ionic matrix

CZE runs with tryptophan enantiomers, added to a mixture of products formed by Maillard's reaction of glycine and xylose [51], were performed to assess some of the potentialities of the present fiber-coupled DAD in a combination with a relevant data processing procedure in identifying enantiomers present in complex ionic matrices. Here, our attention was focused on a situation in which one of the enantiomers (present on a trace concentration level in the

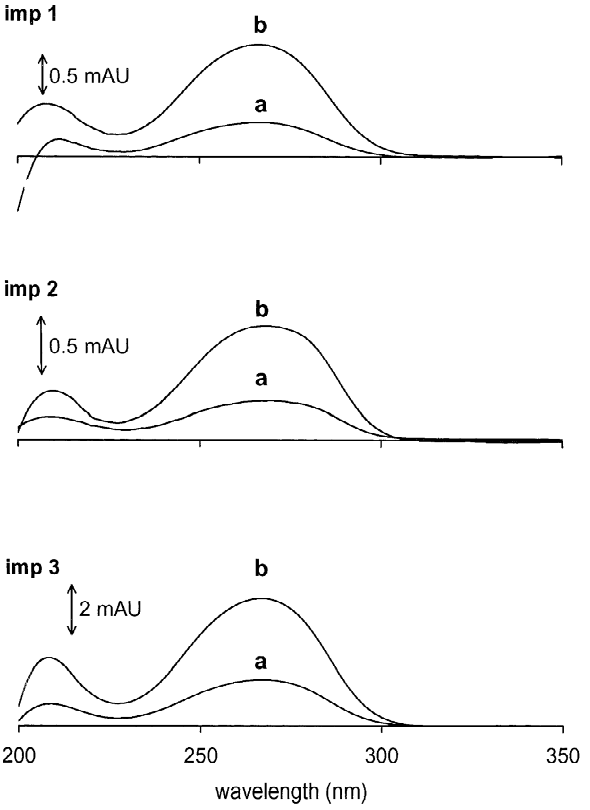

Fig. 6. Spectra of impurities present in the asulam preparation as obtained by DAD in the CZE runs with different carrier electrolytes in the detection column of the tandem (see Fig. 5a and b). (a) The spectra (background corrected and smoothed) acquired in the electrolyte system no. 1a (Table 1). (b) The spectra (background corrected and smoothed) acquired in the electrolyte system no. 1c (Table 1). In both instances the electrolyte system no. 1a was used in the separation column of the tandem. For further details describing the working conditions see Fig. 5.

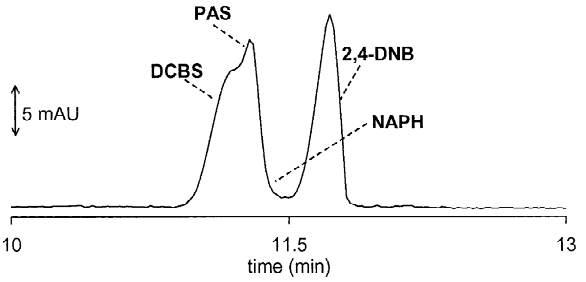

Fig. 7. An electropherogram (225 nm) from the CZE separation of naphthalene-2-sulfonic acid (0.5 μmol/l) from 2,5-dichlorobenzenesulfonic acid (DCBS), *p*-aminosalicylic acid (PAS) and 2,4-dinitrobenzoic acid (2,4-DNB), each at a 100 μmol/l concentration. The separation was carried out in the electrolyte system no. 1b (Table 1) with a 50 μA driving current.

loaded sample) should be identified in a matrix representing a source of spectral disturbances. Two alternative concentration ratios of the tryptophan enantiomers were evaluated as documented by illustrative electropherograms in Fig. 10a and b. The acquired spectral data were processed by FSW-TTFA. The corresponding plots of logarithmically transformed Pearson correlation coefficients (Fig. 10c and d) clearly identified the migration positions of the enantiomers. Here, only one of the matrix constituents (x in Fig. 10) provided a false spectral match. This false was eliminated in a subsequent data processing step with the aid of the TTFA procedure.

Table 3
Relative contents of anionic impurities as determined with the aid of different carrier electrolyte solutions in the detection column of the tandem

Peak[a]	Electrolyte system 1a/1a[a]		Electrolyte system 1a/1c[a]	
	Peak area (mAU s)	Relative area[b] (%)	Peak area (mAU s)	Relative area[b] (%)
Asulam	7655.0	–	29,131.0	–
Imp1	4.2	0.06	21.2	0.07
Imp2	6.6	0.08	26.9	0.09
Imp3	36.9	0.48	138.5	0.48
x	6.7	0.09	–	–

[a] See the electropherograms in Fig. 5; the carrier electrolyte in the separation column/carrier electrolyte in the detection column; for the compositions of the carrier electrolytes see Table 1.

[b] The peak area related to the peak area of asulam.

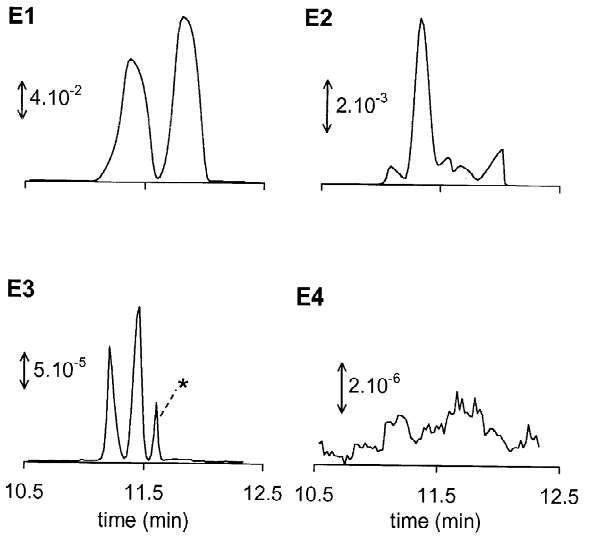

Fig. 8. An analysis of the 3D data as obtained by DAD in the CZE run shown in Fig. 7. The spectral data were processed by FSW-EFA. E1–E4, time plots of the eigenvalues. See the relevant text for further details.

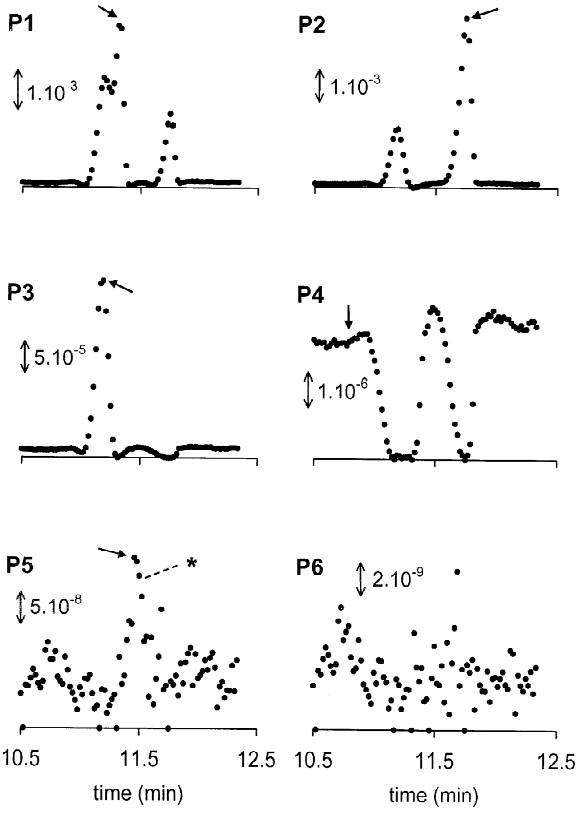

Fig. 9. An analysis of the 3D data as obtained by DAD in the CZE run shown in Fig. 7. The spectral data were processed by OPA. P1–P6, dissimilarity time plots. For further details see the text.

4. Conclusions

Diode array detection, coupled to a 320 μm I.D. fused-silica capillary tube by optical fibers, provided 0.2–1 μmol/l concentration detectabilities for the CZE analytes loaded into the separation system in 200-nl volumes. Although these values are 3–5 times higher than those we could reach under similar working conditions by fixed-wavelength, on-column CE photometric absorbance detectors [35–39,41,42], they are well below those considered in the literature [2] as current concentration limits for on-column photometric absorbance detectors in 50–75 μm I.D. fused-silica capillary tubes. This fact can be, undoubtedly, ascribed to a 250-μm mean effective pathlength in the detection cell on the 320 μm I.D. tube [2] and, in addition, to an inherently higher photon flux through such a cell (leading to reduced effects of shot noise on the detection [2,10,43]).

Confirmations of the identities of the test analytes based on the data acquired by the present DAD system were possible when their concentrations in the loaded samples were 1–5 μmol/l. The use of appropriate data processing procedures was very beneficial at such concentrations as documented, for example, by the data summarized in Table 2.

The tandem-coupled columns offer practical means for performing CZE runs in which the separating and detection conditions are selected, within certain limits, independently. We showed benefits of the tandem in improving the conditions for the data acquisition by concentrating the analytes before their entrance into the cell of the fiber-coupled DAD detector. For obvious reasons, a desired detection and/or identification effect could be reached only when adequate resolutions in the separation column of the tandem were provided (Fig. 5).

The results of experiments performed with

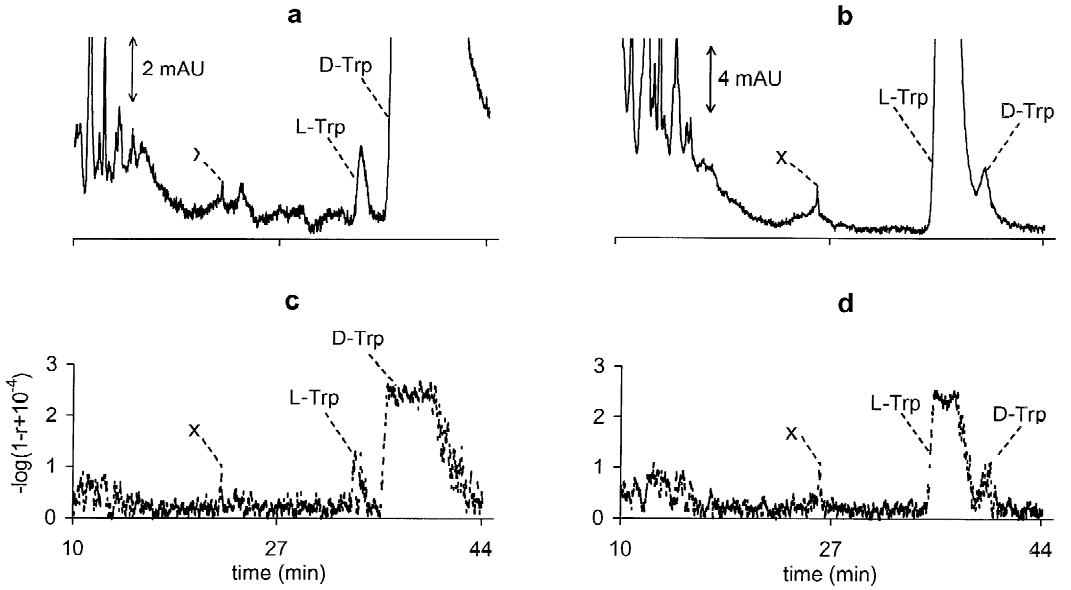

Fig. 10. Spectral identifications of tryptophan enantiomers added to a mixture of products of Maillard's reaction. (a) An electropherogram (220 nm) from the CZE run with the sample containing L-tryptophan (6 μmol/l) and D-tryptophan (7.5 m*M*) in a concentration ratio of 1:1250; (b) the run as in (a) only L-tryptophan (0.85 m*M*) and D-tryptophan (6 μmol/l) were loaded in a 141:1 concentration ratio. (c, d) Time courses of the logarithmically transformed values of the Pearson correlation coefficients as provided by the FSW-TTFA processing of the spectra acquired in the runs (a) and (b), respectively. The CZE separations were carried out in the electrolyte system no. 2 (Table 1) with the driving current stabilized at 50 μA.

tryptophan enantiomers (Fig. 10) indicate that by on-line coupling the present CZE–DAD combination with ITP sample pretreatment, a powerful CE tool for the detection and/or identification of trace enantiomers present in complex biomatrices can be obtained. Our previous work performed along this line [53,54] clearly support such an expectation.

Acknowledgements

This work was supported by a grant from the Slovak Grant Agency for Science under the project no. 1/7247/20. Young scientist grants awarded by the Rector of Comenius University to S.S., M.D., and M.M. (117/2002/UK, 83/2002/UK and 112/2002/UK, respectively) are acknowledged. The authors thank J&M (Aalen, Germany) for providing a TIDAS multiwavelength photometric absorbance detector.

References

[1] S.J. Kok, N.H. Velthorst, C. Gooijer, U.A.T. Brinkman, Electrophoresis 19 (1998) 2753.
[2] S.L. Pentoney Jr., J.V. Sweedler, Optical detection techniques for capillary electrophoresis, in: J.P. Landers (Ed.), Handbook of Capillary Electrophoresis, CRC, Boca Raton, FL, 1997, p. 379, Chapter 12.
[3] W. Beck, R. Vanhoek, H. Engelhardt, Electrophoresis 14 (1993) 540.
[4] D.N. Heiger, P. Kaltenbach, H.J.P. Sievert, Electrophoresis 15 (1994) 1234.
[5] P. Kaltenbach, Hewlett-Packard J. 46 (1995) 20.
[6] T.E. Wheat, F.M. Chiklis, K.A. Lilley, J. Liq. Chromatogr. 18 (1995) 3643.
[7] E. Jellum, H. Dollekamp, A. Brunsvig, R. Gislefoss, J. Chromatogr. B 689 (1997) 155.
[8] F. Tagliaro, G. Manetto, F. Crivellente, D. Scarcella, M. Marigo, Forensic Sci. Int. 92 (1998) 201.
[9] V. Virtanen, G. Bordin, J. Liq. Chromatogr. 21 (1998) 3087.
[10] E.T. Bergstrom, D.M. Goodall, B. Pokric, N.M. Allinson, Anal. Chem. 71 (1999) 4376.
[11] E. Dabek-Zlotorzynska, E.P.C. Lai, J. Chromatogr. A 853 (1999) 487.
[12] S. Heitmeier, G. Blaschke, J. Chromatogr. B 721 (1999) 93.

[13] A.T. Timpermann, J.V. Sweedler, Analyst 121 (1996) 45R.
[14] P.A. Walker, W.K. Kowalchyk, M.D. Morris, Anal. Chem. 67 (1995) 4255.
[15] P.A. Walker, M.D. Morris, J. Chromatogr. A 805 (1998) 269.
[16] R.A. Kautz, M.E. Lacey, A.M. Wolters, F. Foret, A.G. Webb, B.L. Karger, J.V. Sweedler, J. Am. Chem. Soc. 123 (2001) 3159.
[17] A.M. Wolters, D.A. Jayawickrama, C.K. Larive, J.V. Sweedler, Anal. Chem. 74 (2002) 2306.
[18] J.P. Chervet, R.E.J. Vansoest, M. Ursem, J. Chromatogr. 543 (1991) 439.
[19] F.I. Onuska, K.A. Terry, J. Microcol. Sep. 5 (1993) 255.
[20] T.S. Wang, J.H. Aiken, C.W. Huie, R.A. Hartwick, Anal. Chem. 63 (1991) 1372.
[21] J.A. Taylor, E.S. Yeung, J. Chromatogr. 550 (1991) 831.
[22] C.T. Culbertson, J.W. Jorgenson, J. Microcol. Sep. 11 (1999) 652.
[23] HP-3D Capillary Electrophoresis System. Technical Description, Publication No. 12-5965-6512E, Hewlett-Packard, Waldbronn, 1996.
[24] J.C. Reijenga, E. Kenndler, J. Chromatogr. A 659 (1994) 403.
[25] A.E. Bruno, E. Gassmann, N. Pericles, K. Anton, Anal. Chem. 61 (1989) 876.
[26] F. Foret, M. Deml, V. Kahle, P. Boèek, Electrophoresis 7 (1986) 430.
[27] F. Foret, D.P. Kirby, P. Vouros, B.L. Karger, Electrophoresis 17 (1996) 1829.
[28] F. Foret, H.H. Zhou, E. Gangl, B.L. Karger, Electrophoresis 21 (2000) 1363.
[29] H. Ludi, E. Gassmann, H. Grossenbacher, W. Marki, Anal. Chim. Acta 213 (1988) 215.
[30] B.S. Seidel, W. Faubel, J. Chromatogr. A 817 (1998) 223.
[31] P. Lindberg, A. Hanning, T. Lindberg, J. Roeraade, J. Chromatogr. A 809 (1998) 181.
[32] B.M. Xin, M.L. Lee, Electrophoresis 20 (1999) 67.
[33] F.E.P. Mikkers, F.M. Everaerts, T.P.E.M. Verheggen, J. Chromatogr. 169 (1979) 11.
[34] F.E.P. Mikkers, F.M. Everaerts, T.P.E.M. Verheggen, J. Chromatogr. 169 (1979) 1.
[35] D. Kaniansky, M. Masár, V. Madajová, J. Marák, J. Chromatogr. A 677 (1994) 179.
[36] D. Kaniansky, M. Masár, J. Marák, V. Madajová, F.I. Onuska, J. Radioanal. Nucl. Chem. 208 (1996) 331.
[37] D. Kaniansky, E. Krčmová, V. Madajová, M. Masár, J. Marák, F.I. Onuska, J. Chromatogr. A 772 (1997) 327.
[38] D. Kaniansky, J. Marák, M. Masár, F. Iványi, V. Madajová, Šimuničová, J. Chromatogr. A 772 (1997) 103.
[39] D. Kaniansky, E. Krčmová, V. Madajová, M. Masár, Electrophoresis 18 (1997) 260.
[40] D. Kaniansky, M. Masár, J. Bielčíková, J. Chromatogr. A 792 (1997) 483.
[41] M. Masár, D. Kaniansky, V. Madajová, J. Chromatogr. A 724 (1996) 327.
[42] M. Masár, D. Kaniansky, J. Capillary Electrophor. 3 (1996) 165.
[43] C.D. Flint, P.R. Grochowicz, C.F. Simpson, Anal. Proc. 31 (1994) 117.
[44] M. Danková, S. Strašík, M. Molnárová, D. Kaniansky, J. Marák, J. Chromatogr. A 916 (2001) 143.
[45] B.G.M. Vandeginste, D.L. Massart, L.M.C. Buydens, S. De Jong, P.J. Lewi, J. Smeyers-Verbeke, Handbook of Chemometrics and Qualimetrics, Part B, Elsevier, Amsterdam, 1998.
[46] D. Kaniansky, Ph.D. Thesis, Comenius University, Bratislava, 1981.
[47] P. Havaši, D. Kaniansky, J. Chromatogr. 325 (1985) 137.
[48] K. De Braekeleer, A. de Juan, D.L. Massart, J. Chromatogr. A 832 (1999) 67.
[49] J.A. Gilliard, C. Ritter, J. Chromatogr. A 758 (1997) 1.
[50] A.G. Frenich, J.R. Torres-Lapasio, K. De Braekeleer, D.L. Massart, J.L.M. Vidal, M.M. Galera, J. Chromatogr. A 855 (1999) 487.
[51] S. Strašík, M.Sc. Thesis, Comenius University, Bratislava, 1999.
[52] L. Valtcheva, J. Mohammad, G. Pettersson, S. Hjerten, J. Chromatogr. 638 (1993) 263.
[53] M. Danková, D. Kaniansky, S. Fanali, F. Iványi, J. Chromatogr. A 838 (1999) 31.
[54] S. Fanali, C. Desiderio, E. Ölvecká, D. Kaniansky, M. Vojtek, A. Ferancová, J. High Resolut. Chromatogr. 23 (2000) 531.